The Fusogen EFF-1 Controls Sculpting of Mechanosensory Dendrites

Meital Oren-Suissa *et al.*

Science **328**, 1285 (2010);
DOI: 10.1126/science.1189095

The Fusogen EFF-1 Controls Sculpting of Mechanosensory Dendrites

Meital Oren-Suissa,[1] David H. Hall,[2] Millet Treinin,[3] Gidi Shemer,[1]*† Benjamin Podbilewicz[1]†

The mechanisms controlling the formation and maintenance of neuronal trees are poorly understood. We examined the dynamic development of two arborized mechanoreceptor neurons (PVDs) required for reception of strong mechanical stimuli in *Caenorhabditis elegans*. The PVDs elaborated dendritic trees comprising structural units we call "menorahs." We studied how the number, structure, and function of menorahs were maintained. EFF-1, an essential protein mediating cell fusion, acted autonomously in the PVDs to trim developing menorahs. *eff-1* mutants displayed hyperbranched, disorganized menorahs. Overexpression of EFF-1 in the PVD reduced branching. Neuronal pruning appeared to involve EFF-1–dependent branch retraction and neurite-neurite autofusion. Thus, EFF-1 activities may act as a quality control mechanism during the sculpting of dendritic trees.

Morphologies of dendritic trees vary from one neuronal type to another, and the pattern of these arbors determines the manner in which a neuron processes its synaptic or sensory input. However, little is known regarding the mechanisms controlling the outgrowth and maintenance of dendritic trees (*1*–*4*). Two mechanoreceptors in *Caenorhabditis elegans* (PVDR and PVDL; right and left, respectively) are responsible for an avoidance response triggered by strong mechanical stimuli to the body (*5*). The complete neural system of *C. elegans* has been considered to comprise only simple-patterned neurons (*6*). However, recent studies show that the PVDs have a more complex morphology (*7*, *8*).

Here, we established a genetic system to dissect the mechanisms of branch generation and plasticity of arborized neurons in *C. elegans*. To determine branching patterns, we imaged transgenic animals expressing cytoplasmic *ser-2p*::GFP (green fluorescent protein) or plasma membrane DES-2::GFP in the PVDs (table S1). The PVDs contained repetitive structural units reminiscent of multibranched candelabras or menorahs (Fig. 1A). Although the number of menorah branches varied, the menorahs appeared to develop in a stepwise manner from the L2 larva to the adult (fig. S1). The stereotypical menorah structure is likely to form a functional unit necessary for the PVDs mechanosensory activities.

Mutations in the cell fusion gene *eff-1* (*9*, *10*) affected the pattern of PVDs arborization, resulting in disorganized and hyperbranched phenotypes (Fig. 1B). Moreover, *eff-1(ok1021)* mutant animals showed reduced sensitivity to strong mechanical stimuli (53%, $n = 106$) (*11*). To characterize menorah disorganization in *eff-1* mutants, we quantified the number of processes at different degrees of the branching order (primary to senary branches; Fig. 1C and fig. S2). The frequency of secondary and tertiary branching was doubled in the *eff-1(hy21)* mutant compared with wild type. The *eff-1(hy21)* mutant had a strong branching phenotype, whereas the *oj55* mutant displayed a weaker effect, correlating with their respective epithelial fusion-defective phenotype (figs. S2 and S5). In wild-type menorahs, most sprouting of branches and bending of tertiary processes occurred at right angles to the branches of origin (Fig. 1A). In contrast, *eff-1(hy21)* mutant menorahs showed varying branching angles (Fig. 1B). We observed in the mutant a 10-fold increase in the number of branches sprouting from the secondary branch (Fig. 1D) and a 20-fold increase in the number of branches that erred and turned back 180° (Fig. 1E). These phenotypes suggest that EFF-1 sculpts and maintains right-angle nonoverlapping branches.

Cell-specific expression of *eff-1* in the PVDs (*des-2p::eff-1*) partially rescued neuronal *eff-1* phenotypes (Fig. 2C). In contrast, PVD patterning defects were not rescued by expression of *eff-1* in the neighboring epidermal tissue (fig. S3; *dpy-7p::eff-1*). In *eff-1(hy21)* mutants expressing *eff-1* in both neural and epidermal tissues (*des-2p::eff-1+dpy-7p::eff-1*), the rescue was not significantly stronger than the rescue observed with only the PVD-specific *des-2p::eff-1* (fig. S3). These rescue experiments, together with expression of EFF-1::GFP in the PVDs (fig. S4), provide evidence that *eff-1* controls branching cell autonomously. Moreover, *eff-1* overexpression in the PVDs of wild-type animals reduced branching (Fig. 2D).

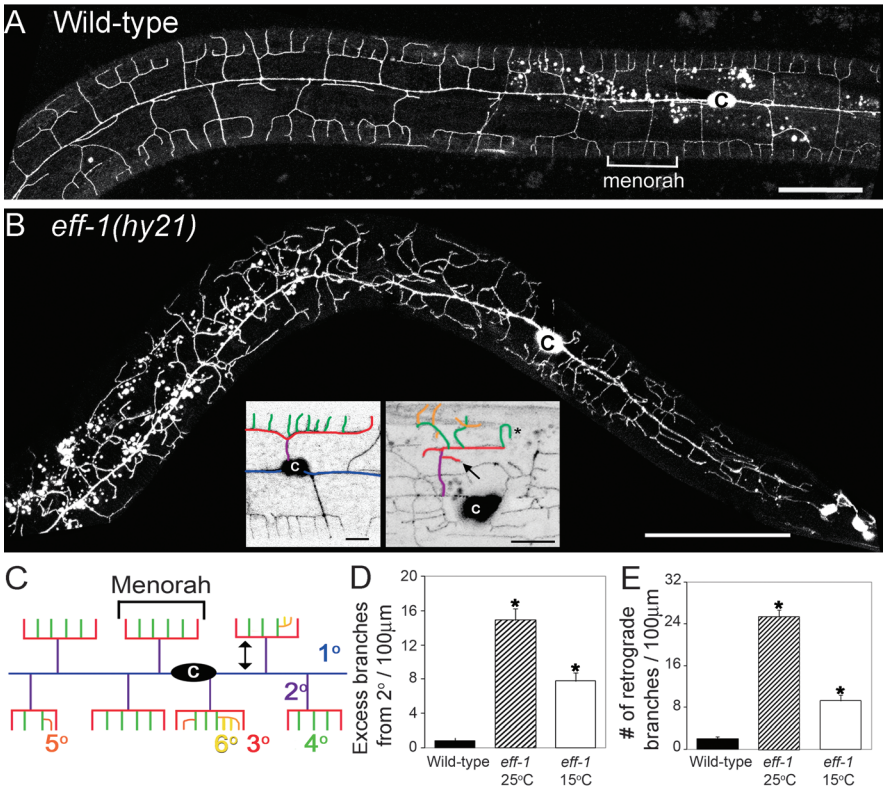

Fig. 1. PVD menorah sculpting by EFF-1. "c" denotes cell body, small droplets are autofluorescent gut granules, anterior is left, and dorsal is up. (**A**) Full stereotypic arborization pattern in young adult. (**B**) PVD in *eff-1(hy21)* showing disorganized menorahs. (Insets) Wild-type menorah (left) and *eff-1(hy21)* mutant (right) with excess branching from secondary stem (arrow) and abnormal retrograde migration of quaternary branch (asterisk). Scale bars represent 50 µm [(A) and (B)] and 10 µm [(B) insets]. (**C**) Menorah pattern map [primary to senary (1° to 6°) are blue, purple, red, green, orange, and yellow, respectively]. (**D**) Excess bifurcations from secondary stems in *eff-1(hy21ts)*. (**E**) Increased retrograde branches in *eff-1(hy21ts)*. In (D) and (E), $^*P < 0.0001$, two-tailed *t* test. Data are mean ± SE. All experiments were compared with wild type at 20°C, $n = 20$, 260 menorahs. *hy21* at 25°C, $n = 6$, 355 menorahs. *hy21* at 15°C, $n = 10$, 322 menorahs. *n*, number of animals analyzed. We also performed a one-way analysis of variance (ANOVA) followed by Dunnett's multiple comparison test (*11*).

[1]Department of Biology, Technion-Israel Institute of Technology, Haifa 32000, Israel. [2]Center for *C. elegans* Anatomy, Dominick P. Purpura Department of Neuroscience, Albert Einstein College of Medicine, New York, NY 10461, USA. [3]Department of Physiology, Hebrew University-Hadassah Medical School, Jerusalem 91120, Israel.

*Present address: Department of Biology, University of North Carolina at Chapel Hill, Chapel Hill, NC 27599, USA. †To whom correspondence should be addressed. E-mail: podbilew@tx.technion.ac.il (B.P.); bishemer@email.unc.edu (G.S.)

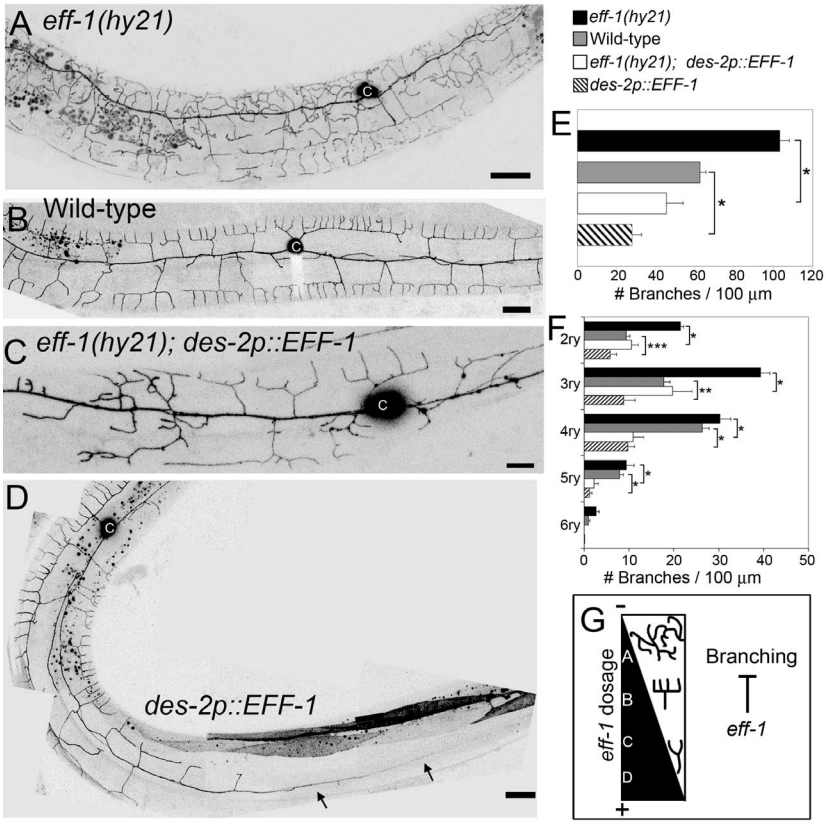

Fig. 2. EFF-1 autonomously rescues PVD arborization and restricts branching. (**A**) *eff-1(hy21)* at 25°C had twice as many secondary and tertiary branches as the wild type. Scale bars represent 10 μm. (**B**) Menorahs in wild-type animals. (**C**) Expression of EFF-1 *(des-2p::EFF-1)* in the PVD in *eff-1(hy21)* mutants at 25°C partially rescued the menorah pattern and reduced the number of branches. (**D**) Overexpression of *des-2p::EFF-1* in wild-type animals caused a menorah gradient starting from the PVD cell body until dendrites disappeared toward the posterior (arrows). (**E**) Apparent EFF-1 dosage–sensitive reduction in branching. $*P < 0.0001$, $**P < 0.001$, $***P < 0.05$, two-tailed *t* test. We also performed ANOVA (*11*). Data are mean ± SE. *eff-1(hy21)*, $n = 6$; number of wild-type animals, $n = 6$; *eff-1(hy21);des-2p::EFF-1*, 25°C, $n = 5$; *des-2p::EFF-1*, $n = 6$. (**F**) Quantification of the number of secondary to senary branches showed that secondary and tertiary branches were doubled in the mutant compared with wild type and that secondary to quinary branches were reduced when EFF-1 was expressed ectopically in the PVD. (**G**) A model for the maintenance of PVD branching in an *eff-1* dosage–dependent manner. Low levels of *eff-1* (A) increased the number of PVD branches, and elevated levels of *eff-1* reduced branching (D).

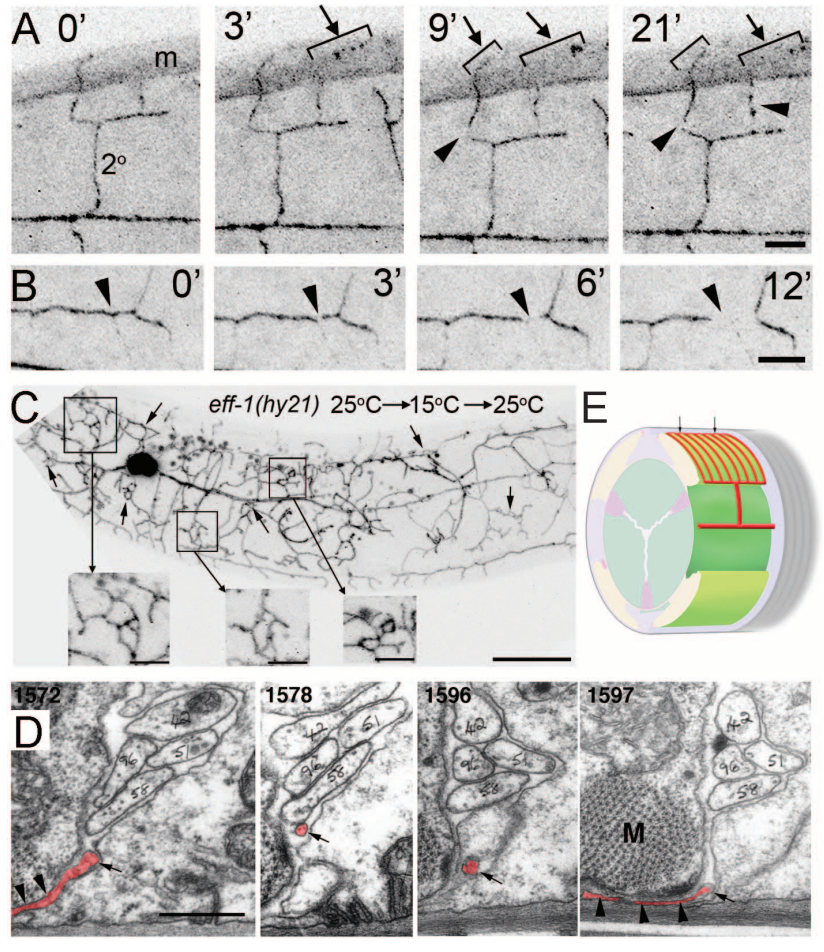

Fig. 3. Dendrite autofusion and fission trim menorahs. Scale bars represent 5 μm, (A) and (B); 20 μm and insets 5 μm, (C); and 0.5 μm, (D). (**A**) Trimming of dendrites that break off (arrows) and fission of branches in *des-2p::EFF-1* animal (arrowheads). m, body wall muscle. (**B**) Fission of a branch in *des-2p::EFF-1* animal (arrowhead). (**C**) *eff-1(hy21ts)* animal grown at 25° downshifted to 15° for 4 hours and then upshifted to 25° for 2 hours. Loops can be seen (arrows and insets). (**D**) Four TEM prints from wild-type animal "N2U" (*6*) showing the route of a PVD fusion process at the edge of the ventral nerve cord. Prints 1572 and 1597 show quaternary dendrites (arrowheads, red pseudocolor) passing between a thin layer of hypodermis and body wall muscle (M). PVD branch emerged from one quaternary dendrite at 1572, joined the minor fascicle of the ventral cord between 1578 and 1592, and ran ventralward to autofuse with another quaternary dendrite at 1596 and 1597 (arrows). Whereas this fusion process of PVD spans about 3 μm along the anterior-posterior axis, the marked neuron processes (42, 51, 58, and 96) were traced for thousands of serial sections back to their cell bodies. Dorsal is down (fig. S9; www.wormimage.org). (**E**) Cartoon representing one menorah (red) with eight terminal dendrites autofused along the dorsal midline (arrows).

The remaining branches were organized in a gradient starting from the cell body toward the head and tail, where no branches could be observed. Thus, *eff-1* may play a role in mechanosensory neurons restricting branching in a dosage-dependent manner to produce dendrite simplification (Fig. 2G).

The absence of excess branching in wild-type animals may reflect a situation where only the appropriate branches initiate outgrowth. Alternatively, an excess of branches may be generated and extended but at some later point undergo retraction, pruning, or fusion to repair branching errors. To determine how EFF-1 restricts branching, we followed the behavior of branches by using three-dimensional (3D) live-imaging confocal microscopy in wild-type animals overexpressing *des-2p::eff-1*. The tips of tertiary to senary menorah branches first contacted the muscle cells, and then the dendrites detached from the menorahs by fission events (Fig. 3A; arrowheads) causing spontaneous dendrite break-off (Fig. 3B; arrowheads). Thus, following dynamic outgrowth, fission events eliminate extra branches.

To further analyze *eff-1*–dependent remodeling of menorahs, we grew the *eff-1(hy21ts)* worms at the restrictive temperature and shifted them to the permissive temperature in the early L4 stage. The defective arborization pattern was static at the nonpermissive temperature. Four hours after downshifting to the permissive temperature, we observed branches that met, touched, and retracted. Some branches appeared to be stably connected, forming loops of different sizes and shapes (43 stable loops, $n = 18$; fig. S6). Because EFF-1 is a fusogen, we hypothesized that transient meeting and attachment of branches expressing EFF-1 may have resulted in loop formation because of interbranch fusion. To distinguish between interbranch fasciculation and fusion, we analyzed the 3D structure of the loops by generating confocal z stacks, projections, and rotations. The loops were stably connected over time (55 loops, $n = 18$ animals; movie S1). Next, we imaged DES-2::GFP in loops and found that fluorescent particles moved freely through them. To test whether the loops resulted from *eff-1* activity, we incubated temperature-sensitive mutants at the restrictive temperature to generate hyperbranching, then we shifted them to the permissive temperature to induce expression of active EFF-1. After generating loops for 3.5 hours, we upshifted the worms back to the restrictive temperature to stabilize the loops (fig. S8). We obtained a two- to threefold increase in the number of loops (119 stable loops in $n = 16$ animals; Fig. 3C). We also observed symmetric fluorescence recovery of photobleached areas within the loops (fig. S7 and movie S2), indicating that the loops are continuous. Thus, *eff-1* induces loop formation by neurite autofusion and/or fasciculation.

To further demonstrate that neurites can fuse with each other, we turned to higher resolution images of menorah branches and membranes. By using archival serial section transmission electron micrographs [TEMs (*6*)], we identified arborizations derived from the PVDs. In transverse sections of an adult hermaphrodite (N2U), 30- to 80-nm-diameter branches sandwiched between the body wall muscles and the hypodermis were observed (Fig. 3D, arrowheads). We reconstructed parallel neurites corresponding to the quaternary branches of a menorah from serial sections (Fig. 3E and figs. S9 to S11). In 10 examples of PVDs and FLPL/R (highly arborized neurons anterior to the PVDs), we found 2 to 12 branches fusing at the midline and forming fused longitudinal processes (Fig. 3, D and E, arrows). In no cases did we observe distal dendrites fasciculate; instead these fused if they reached one another. Thus, neurite-neurite autofusion plays a role in PVD and FLP arborization.

In addition to loop formation, dendrites were highly dynamic, erring, growing, and retracting in wild-type worms (Fig. 4A and movie S3). PVDs overexpressing *eff-1* showed similar retractions but, unlike in the wild type, showed limited branch growth (Fig. 4, B and C). Similarly, when *eff-1(hy21ts)* animals were downshifted from the restrictive to the permissive temperature, we observed a 20-fold increase in the number of retracting branches and a 5-fold reduction in branch growth compared with *eff-1* mutants at 25°C (Fig. 4, D to G, and movie S1). In contrast, upshifting *eff-1(hy21ts)* worms resulted in excess neurite growth

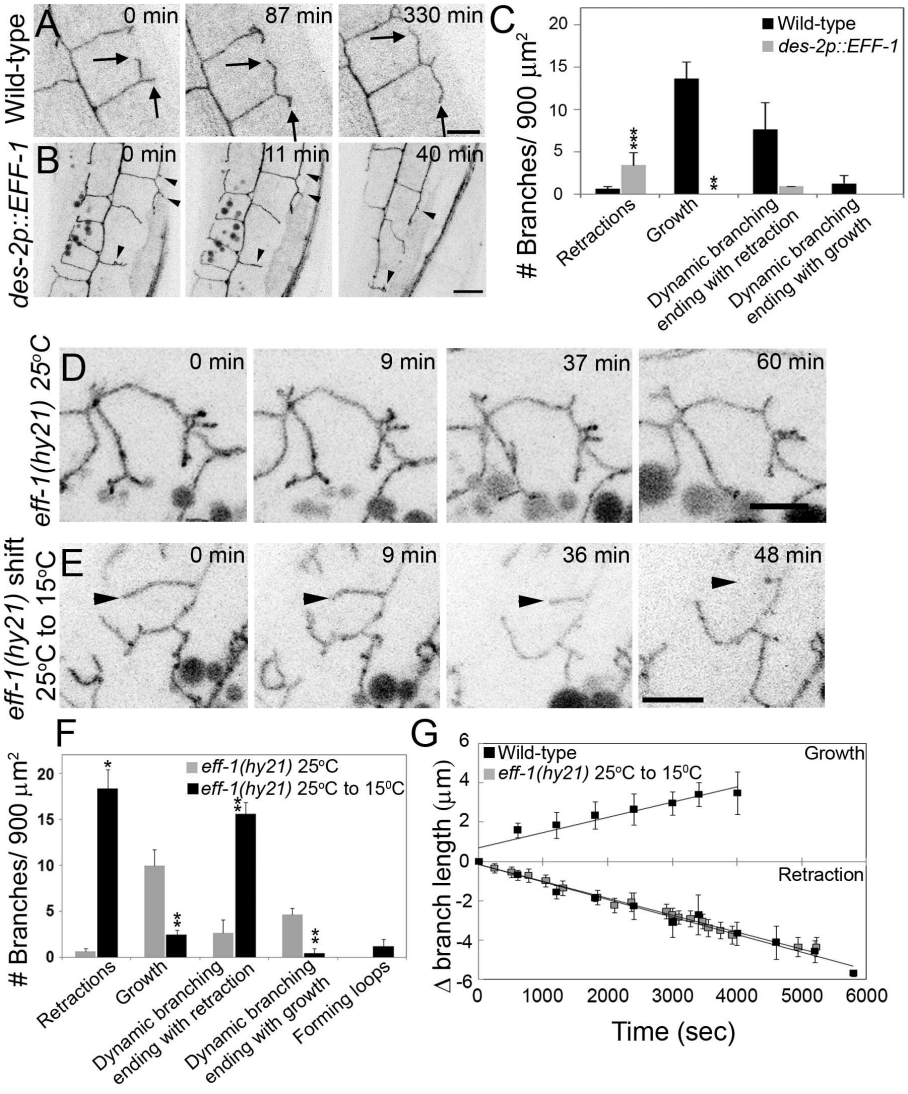

Fig. 4. EFF-1–dependent retraction of branches. (**A**, **B**, **D**, and **E**) Time-lapse confocal projections of L4 and young-adult animals. (A) Growth of a wild-type menorah (movie S3). Growing tertiary branches (arrows). (B) Retraction of branches in *des-2p::EFF-1* animal (arrowheads). (**C**) Number of branches growing and retracting in *des-2p::EFF-1* and wild type. Branches first showed dynamic movements but eventually either shortened or lengthened (dynamic branching ending with growth or retraction). $^{**}P < 0.01$, $^{***}P < 0.05$, two-tailed *t* test. Data shown as mean ± SE. Wild type, $n = 3$; *des-2p::EFF-1*, $n = 2$. (D) L4 *eff-1(hy21ts)* at 25°C, branches were static. (E) Retracting branch in L4 *eff-1(hy21ts)* grown at 25°C and shifted to 15°C for 4 hours (arrowhead; movie S1). (**F**) Number of branches showing growth and retraction in *eff-1(hy21)* grown at 25°C and downshifted as in (E). $^{*}P < 0.001$, $^{**}P < 0.01$, two-tailed *t* test. Data are mean ± SE. *eff-1(hy21)* 25°C, $n = 3$; *eff-1(hy21)* 25° to 15°C, $n = 4$ animals. (**G**) Wild-type branches grew (0.8 nm/s; $N = 5$ branches) and retracted (0.9 nm/s; $N = 3$ branches). In *eff-1(hy21)* temperature-shifted animals, branches retracted (0.9 nm/s; $N = 10$ branches). Data are mean ± SE. Scale bars represent 5 µm.

(Fig. 4F). Thus, we propose a model in which EFF-1 autonomously induces retraction of branches to simplify menorahs.

EFF-1 is both a sculptor of epithelial organs by cell fusion (*10*) and a menorah sculptor by controlling dendrite bending, retraction, and fusion. The activities of this fusogen may be due to its ability to induce membrane curvature, a process that is thought to constitute a major driving force in membrane fusion and fission (*12*–*14*). Proteins capable of bending membranes, such as atlastins (*15*, *16*) and dynamins (*17*), can induce tubulation, fusion, and fission (*12*, *13*). Three mechanistic principles may form and maintain branched tubes in the cytoplasm and in extracellular branched filopodia or neuronal arbors such as menorahs: first, assembly of specialized proteins on membranes; second, membranous tube formation involving growth and bifurcation of tubes; and third, membrane bending followed by membrane fusion and fission restricts excessive branching. How can EFF-1 control mechanistically different processes such as dendrite fusion and retraction? Different isoforms and interactions may account for diverse activities. For example, trans interactions between EFF-1 on dendrites will cause autofusion, whereas assembly of large EFF-1 complexes on dendrites may induce actin-mediated retraction.

Note added in proof: After we submitted this report, Ghosh-Roy *et al.* (*18*) showed that axotomized PLM sensory neurons fail to reconnect in *eff-1* mutants.

References and Notes

1. E. K. Scott, L. Luo, *Nat. Neurosci.* **4**, 359 (2001).
2. W. B. Grueber, Y. N. Jan, *Curr. Opin. Neurobiol.* **14**, 74 (2004).
3. D. M. Tobin, C. I. Bargmann, *J. Neurobiol.* **61**, 161 (2004).
4. C. Jinghong, T. Guoxi, *Brain Res.* **846**, 243 (1999).
5. J. C. Way, M. Chalfie, *Genes Dev.* **3**, (12A), 1823 (1989).
6. J. G. White, E. Southgate, J. N. Thomson, S. Brenner, *Philos. Trans. R. Soc. London Ser. B* **314**, 1 (1986).
7. E. L. Tsalik *et al.*, *Dev. Biol.* **263**, 81 (2003).
8. S. Halevi *et al.*, *EMBO J.* **21**, 1012 (2002).
9. W. A. Mohler *et al.*, *Dev. Cell* **2**, 355 (2002).
10. B. Podbilewicz *et al.*, *Dev. Cell* **11**, 471 (2006).
11. Materials and methods are available as supporting material on *Science* Online.
12. S. Martens, H. T. McMahon, *Nat. Rev. Mol. Cell Biol.* **9**, 543 (2008).
13. L. V. Chernomordik, M. M. Kozlov, *Annu. Rev. Biochem.* **72**, 175 (2003).
14. A. Sapir *et al.*, *Dev. Cell* **12**, 683 (2007).
15. G. Orso *et al.*, *Nature* **460**, 978 (2009).
16. J. Hu *et al.*, *Cell* **138**, 549 (2009).
17. P. V. Bashkirov *et al.*, *Cell* **135**, 1276 (2008).
18. A. Ghosh-Roy, Z. Wu, A. Goncharov, Y. Jin, A. D. Chisholm, *J. Neurosci.* **30**, 3175 (2010).

19. We thank A. Fire for vectors; N. Assaf and T. Gattegno for *eff-1* alleles; E. Shmukler for preliminary phenotypic characterization of the PVD in *eff-1(hy21ts)*; T. Stiernagle and the CGC for nematode strains; J. White and J. Hodgkin for donation of the MRC/LMB archival prints to DHH; C. Crocker for TEM cartoon; and O. Avinoam, D. Cassel, M. Kozlov, A. Sapir, and I. Yanai for critically reading the manuscript. Supported by grants from the FIRST program of the Israel Science Foundation (ISF 1542/07 to B.P.), ISF 493/01-16.6 to M.T., and NIH RR12596 (WormImage Web site) to D.H.H.

Supporting Online Material

www.sciencemag.org/cgi/content/full/science.1189095/DC1
Materials and Methods
Figs. S1 to S11
Table S1
References
Movies S1 to S3

4 March 2010; accepted 26 April 2010
Published online 6 May 2010;
10.1126/science.1189095
Include this information when citing this paper.

Induction of Fear Extinction with Hippocampal-Infralimbic BDNF

Jamie Peters,[1] Laura M. Dieppa-Perea,[1] Loyda M. Melendez,[2] Gregory J. Quirk[1]*

The extinction of conditioned fear memories requires plasticity in the infralimbic medial prefrontal cortex (IL mPFC), but little is known about the molecular mechanisms involved. Brain-derived neurotrophic factor (BDNF) is a key mediator of synaptic plasticity in multiple brain areas. In rats subjected to auditory fear conditioning, BDNF infused into the IL mPFC reduced conditioned fear for up to 48 hours, even in the absence of extinction training, which suggests that BDNF substituted for extinction. Similar to extinction, BDNF-induced reduction in fear required *N*-methyl-D-aspartate receptors and did not erase the original fear memory. Rats failing to learn extinction showed reduced BDNF in hippocampal inputs to the IL mPFC, and augmenting BDNF in this pathway prevented extinction failure. Hence, boosting BDNF activity in hippocampal-infralimbic circuits may ameliorate disorders of learned fear.

Extinction of conditioned fear forms a new memory in the infralimbic medial prefrontal cortex (IL mPFC) that is critical for the retrieval of extinction (*1*, *2*). IL single-unit responses correlate with the successful retrieval of such extinction memories (*3*), and IL stimulation strengthens these memories (*3*). Consolidation of extinction requires plasticity within the IL mPFC, which in turn depends on *N*-methyl-D-aspartate (NMDA) receptors, mitogen-activated protein kinase, and protein synthesis (*2*, *4*). Understanding the molecular mechanisms that support this extinction-related plasticity could lead to pharmacological approaches for enhancing extinction memory, which might facilitate the treatment of anxiety disorders.

[1]Department of Psychiatry and Department of Anatomy and Neurobiology, University of Puerto Rico School of Medicine, San Juan, PR 00936, USA. [2]Department of Microbiology, University of Puerto Rico School of Medicine, San Juan, PR 00936, USA.

*To whom correspondence should be addressed. E-mail: gjquirk@yahoo.com

Epigenetic regulation within the IL mPFC of the gene encoding BDNF correlates with fear extinction (*5*). Because BDNF is a major molecular mediator of memory consolidation (*6*), we hypothesized that BDNF is responsible for consolidating extinction memory within the IL mPFC. If true, it should be possible to enhance extinction via direct application of BDNF to the IL mPFC. Accordingly, rats were subjected to auditory fear conditioning and, the following day, received bilateral IL mPFC infusion of human recombinant BDNF protein (0.75 μg per side) 60 min before extinction training. Conditioned freezing in BDNF-treated rats was significantly reduced relative to saline-infused rats (main effect of drug $F_{1,14} = 28.359$, $P < 0.001$, Fig. 1A; for suppression of food seeking, see fig. S1). This effect persisted in an extinction test the following day (day 3, main effect of drug $F_{1,14} = 11.029$, $P = 0.005$, Fig. 1A), which indicated that BDNF strengthened extinction memory.

Freezing was significantly reduced in BDNF rats from the first extinction trial [$t(14) = 3.335$, $P = 0.005$], which suggested that BDNF reduced fear independent of extinction training. We therefore repeated the previous experiment but omitted extinction training from day 2. Conditioned rats were infused with BDNF or saline and returned to their home cages. The following day, freezing was again reduced in BDNF-treated rats from the first trial [$t(10) = 4.476$, $P = 0.001$, Fig. 1B] and throughout the extinction session (main effect of drug $F_{1,10} = 27.220$, $P < 0.001$). Although the effect of BDNF on fear did not require extinction training, it did require conditioning, because BDNF infused 1 day before conditioning did not significantly reduce freezing (Fig. 1C). BDNF infusions did not alter locomotion, anxiety, or motivation to seek food reward (fig. S2, A to C). The lack of effect on conditioning and open-field anxiety suggests that BDNF infusions did not decrease amygdala activity nonspecifically. Nor could BDNF's effects be attributed to potentiation of latent inhibition, because removing habituation trials did not prevent the effect (fig. S2D).

There are two interpretations for these results. BDNF could inhibit fear expression (similar to extinction), or it could have degraded the original fear memory. To distinguish between these possibilities, we determined the extent to which freezing could be reinstated after unsignaled footshocks, which can reveal the underlying fear memory (*7*). One day after infusions, rats were given extinction training followed by two unsignaled shocks. Replicating our previous experiment, BDNF rats showed reduced fear throughout the extinction session (main effect of drug $F_{1,21} = 7.337$, $P = 0.013$, Fig. 2A). On day 4, however, both saline- and BDNF-treated rats froze equivalently to the tone (78% and 80%, respectively; Fig. 2A), indicating that BDNF left the original fear memory intact. The return of freezing on day 4 was not due